Available online at www.sciencedirect.com
SCIENCE DIRECT
Carbohydrate Polymers 62 (2005) 344–356
Carbohydrate Polymers
www.elsevier.com/locate/carbpol

Free radical degradation of hydroxyethyl cellulose

Stefan Erkselius[a], Ola J. Karlsson[b,*]

[a]Department of Polymer Science and Engineering, Lund University, P.O. Box 124, SE-22100 Lund, Sweden
[b]Department of Physical Chemistry 1, Lund University, P.O. Box 124, SE-22100 Lund, Sweden

Received 21 December 2004; accepted 8 August 2005
Available online 12 October 2005

Abstract

The degradation of hydroxyethyl cellulose (HEC) using sodium persulfate (NaPS) as free radical generator was studied at 60, 70 and 80 °C with different NaPS/HEC ratios. During the degradation reaction samples were withdrawn at regular intervals. The amount of persulfate remaining was analyzed by titration and the evolution of the HEC molecular weight distribution and viscosity was followed using size exclusion chromatography (SEC) and rheology, respectively. The results show how the molecular weight of HEC is decreased by varying the NaPS/HEC ratio, reaction time and temperature. It was found that the NaPS/HEC ratio must be kept low in order to maintain the control of the degradation process, since when the NaPS/HEC ratio was too high the degradation rate of HEC was too fast, and the molecular weight distribution became bimodal. Additionally, the decomposition rate of NaPS was found to be independent of pH in the range between pH 2 and 7.

Keywords: Degradation; Hydroxyethyl cellulose; Sodium persulfate

1. Introduction

A waterborne paint is a complex blend of latex particles, surfactants, thickeners, fillers, pigments, etc. where each additive contributes to the final coating. The use of hydroxyethyl cellulose (HEC) as a stabilizer and thickener in paint formulations is well established and HEC is normally added as an additive during the paint manufacturing in order to achieve the desired rheological effects, i.e. thixotropic behavior during application of the coating (Schwartz & Baumstark, 2001; Warson & Finch, 2001). The main thickener mechanisms of HEC in coatings are firstly through its solution properties, i.e. the rheology of a polymer in solution, and secondly through its adsorption properties, i.e. train and loops on polymer particles and pigments particles as well as limited bridging between various colloidal particles in the formulation (Craig, 1986; Schwartz & Baumstark, 2001; Warson & Finch, 2001). Both the solution and adsorption behavior of HEC are determined to a major extent by the molecular weight of the cellulosic backbone together with the HEC molecules' interactions with surfactants in the formulation. One drawback of the conventional surfactants used in latex production and paint formulation is that they cause difficulties in the final coating application, both wet and dry, e.g. foaming during handling and application and water sensitivity of the coating films are problems commonly encountered.

If copolymerizable surfactants were to be used in the emulsion polymerization producing the latex binder this would decrease the amount of surfactants in a paint formulation, thus avoiding or at least decreasing the problems with foam and surfactant migration in the final coating films (Hellgren, Weissenborn, & Holmberg, 1999). Furthermore, in the drive to design environmentally friendly coatings by emulsion polymerization, studies have been performed aiming at partly replacing or fully substituting the conventional synthetic surfactants with amphiliphilic polymers from renewable resources (Annable, Gray, Lovell, Richards, & Satgurnathan, 2004; Craig, 1985; Hsu, Don, & Chiu, 2001; Janssen, Kroon, Kruythoff, & Salomons, 1996; Kiselenko, Berlin, & Chernyak, 1980; Kislenko, Berlin, & Litovchenko, 1998). One interesting candidate as a renewable amphiphilic polymer used as the sole stabilizer during the latex production is the cellulose ether HEC. If this approach could be successfully applied it would not only

* Corresponding author. Tel.: +46 706 308574.
E-mail address: ola.karlsson@fkeml.lu.se (O.J. Karlsson).

0144-8617/$ - see front matter © 2005 Elsevier Ltd. All rights reserved.
doi:10.1016/j.carbpol.2005.08.013

give surfactant-free polymer dispersion, with all its benefits, but simultaneously a binder with attractive rheological properties.

However, due to the type of initiator used, radicals are formed during the polymerization reaction and the cellulose ether macromolecules undergo chain scission and grafting to the polymer backbone (Annable et al., 2004; Craig, 1985; Kiselenko et al., 1980). The graft polymerization is influenced by several parameters, foremost among which are the type of monomer system, the temperature, the initiator concentration, the ratio of the monomer and the type of cellulose ether, the degree of polymerization and degree of substitution of the cellulose ether and the solution viscosity (Craig, 1985; Janssen et al., 1996; Kiselenko et al., 1980). For future exploitation using HEC as a stabilizing protective colloid in emulsion polymerization the kinetics of the HEC degradation reaction must be known in order to control the polymerization process.

In the beginning of the 1980's the paint industry started to investigate the reason for the viscosity decrease seen in latex paints, thickened with cellulose derivatives, during storage. Until then it was believed that the viscosity decrease in paints was caused by cellulolytic enzymes. However, Winters (1980) observed that the interaction between oxidizing and reducing agents was the major cause of the viscosity decrease. Most of the early investigations that were done studying the degradation of the cellulose derivatives in paint were carried out on the final paint. Irwin and Williams (1980) found that of three different methods: acrylamide gel test, hydroxyethyl cellulose solution test, and oxygen reduction potential (ORP) that were used to study the degradation of HEC in latex paints, it was only ORP that could be used as a guideline to predict the viscosity stability of the final paint if the measurements were performed on the raw latex. This indicated that the best way to study the degradation of cellulose derivative was to separate it from the other components in the system and only study the cellulose derivative itself.

Several analytical methods have been reported for studying the degradation of polysaccharides, and especially cellulose derivatives, in aqueous solutions. Rheology methods were used to study the viscosity and intrinsic viscosity (molecular weight) decrease with time (Kislenko & Berlin, 1980; Donescu, Gosa, Diaconescu, Mazare, & Carp, 1981; Kislenko & Kuryatnikov, 2000; Hsu et al., 2001). Kislenko et al. (1980)also used IR spectroscopy to study the formation of carbonyl and carboxyl groups during degradation of HEC. The formation of carbonyl groups could also be analyzed by using UV spectrometric methods, which were used to study the oxidative degradation by the change in carbonyl absorbance (Annable et al., 2004; Donescu et al., 1981). Different size exclusion chromatography methods have been used to study the decrease of molecular weight with time (Annable et al., 2004; Hsu et al., 2001). Also NMR has been used to study the structure of chitosan after it has been degraded using KPS (Hsu et al., 2001). All these studies have in common that the cellulose derivatives were degraded by the persulfate. However, the types of persulfate that have been used were mainly potassium persulfate (KPS) and ammonium persulfate (APS), no studies have been found where sodium persulfate (NaPS) has been used as the initiator.

In the present study we have examined the degradation of HEC in aqueous solutions containing the initiator NaPS in order to be able to control this reaction later during the emulsion polymerization used for latex production. High molecular weight HEC was degraded at various temperatures and concentration ratios of HEC and initiator and the reaction was followed by analyzing the evolution of the HEC molecular weight and the initiator concentration. In this first paper in the series we report the results for the free radical degradation of HEC and in a consecutive second paper we will report on the reaction kinetics and mechanisms obtained in this study.

2. Experimental

2.1. Materials

Natrosol® 250 Hydroxyethyl Cellulose (HEC) GR (Hercules Inc.) was of commercial grade with the moles of substituent combined (MS) of 2.5 and a degree of substitution (DS) of 1.5, see Fig. 1, having an average molecular weight around 300,000 g/mol as reported by the supplier (Hercules, 1997). Sodium persulfate (NaPS) (Aldrich), Hydroquinone (Aldrich), Sodium hydrogen carbonate ($NaHCO_3$) (Merck), Potassium iodide (KI) (BDH), 2-methyl-4-isothiazolin-3-one (Kathon) (Merck), Sodium thiosulfate ($Na_2S_2O_3$) volumetric standard (0.10 N solution in water) (Aldrich), Acetic acid (glacial 100%)

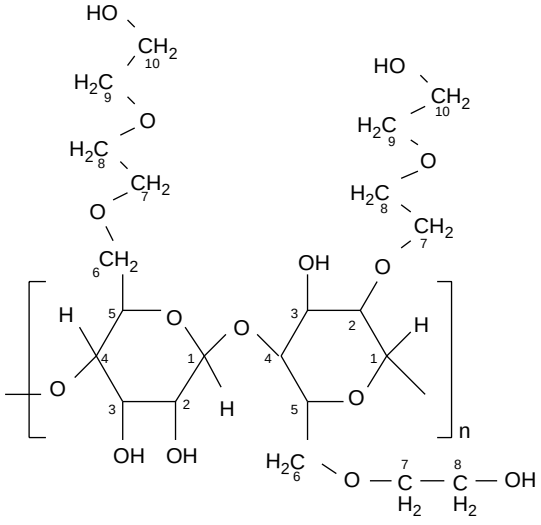

Fig. 1. Schematic structural functions of the used HEC, which moles of substituent combined (MS) of 2.5 and a degree of substitution (DS) of 1.5.

Table 1
Experimental matrix for the degradation of HEC using NaPS

NaPS/HEC weight ratio-'*r*'	Solids content HEC (wt.%)-'s'					
	0.5		2.25		4	
	Experiment	Method	Experiment	Method	Experiment	Method
1	*r*1–*s*0.5–T60	1, 2, 3	*r*1–*s*2.25–T60	1, 2, 4		
	*r*1–*s*0.5–T70	1	*r*1–*s*2.25–T70	1		
	*r*1–*s*0.5–T80	1,2	*r*1–*s*2.25–T80	1		
0.5	*r*0.5–*s*0.5–T60	1, 3	*r*0.5–*s*2.25–T60	1	*r*0.5–*s*4–T60	1
	*r*0.5–*s*0.5–T70	1	*r*0.5–*s*2.25–T70	1	*r*0.5–*s*4–T70	1
	*r*0.5–*s*0.5–T80	1	*r*0.5–*s*2.25–T80	1	*r*0.5–*s*4–T80	1
0.25	*r*0.25–*s*0.5–T60	3				
	*r*0.25–*s*0.5–T80	3				
0.05	*r*0.05–*s*0.5–T60	1, 2, 3, 4	*r*0.05–*s*2.25–T60	1, 2, 3, 4	*r*0.05–*s*4–T60	1, 2, 4
	*r*0.05–*s*0.5–T70	1, 2, 3, 4	*r*0.05–*s*2.25–T70	1	*r*0.05–*s*4–T70	1, 4
	*r*0.05–*s*0.5–T80	1, 2, 3, 4	*r*0.05–*s*2.25–T80	1, 2	*r*0.05–*s*4–T80	1, 2

The NaPS/HEC weight ratios, denoted '*r*', are given in the vertical direction and the different solids content of HEC are given in the horizontal direction. For some of the experiments the molecular weight evolution during the reactions was followed by means of rheology and SEC analysis of samples taken over the course of the reactions and the decomposition of persulfate was followed by iodometric titrations. Analytical methods used: (1) Rheology, (2) Size Exclusion Chromatography, (3) Iodometric titration, (4) Ubbelohde capillary viscometer.

(Merck) and Starch indicator (Aldrich), were all of analytical grade and used as supplied.

2.2. Sample preparation

HEC was dissolved in deionized water at three NaPS/HEC ratios and three different HEC concentrations at three different temperatures (60, 70 and 80 °C), see Table 1. The HEC solutions were prepared in a 2 l double mantled reactor with a constant agitation rate of 100 rpm and a controlled temperature (±0.1 °C). In order to suppress oxygen inhibition, the reactor was repeatedly purged with nitrogen before the system was heated up. When the reactor temperature was stable the NaPS solution was added to the reactor.

Samples for further analysis were withdrawn at different reaction times (0–60 min) as indicated in Table 1. Hydroquinone was added immediately and the samples were placed in an ice bath in order to stop the degradation reaction. In order to protect samples from bacterial growth small amounts of Kathon biocide were added to each sample. The samples were encoded according to the following scheme: NaPS/HEC ratio (*r*), solids content (*s*), temperature (*T*) and time (*t*), e.g. *r*1–*s*0.5–T80–t7 was a sample with an NaPS/HEC ratio of 1 and a solids content of 0.5 wt.% reacted at 80 °C and taken out after 7 min of reaction.

In Table 2 the HEC and NaPS concentrations are given for the experiments presented in Table 1. The HEC concentrations are either based on the number average molecular weight (M_n) or on the average molecular weight per glucose unit (272.3 g/mol) calculated from M_n.

2.3. Analytical methods

The analyses used in this study are presented below and the analytical methods used for each sample are given in Table 1.

Table 2
Concentrations for HEC and NaPS in the different experiments

Experiment	$[HEC]_0$ (g/dm^3)	$[HEC]_{0(glucose)}$ [a] (mol/dm^3)×10^3	$[HEC]_{0(polymer)}$ [b] (mol/dm^3)×10^6	$[NaPS]_0$ [c]	
				(g/dm^3)	(mol/dm^3)×10^3
*r*1–*s*0.5	5	18.4	21.5	5	21.0
*r*0.5–*s*0.5	5	18.4	21.5	2.5	10.5
*r*0.25–*s*0.5	5	18.4	21.5	1.25	5.2
*r*0.05–*s*0.5	5	18.4	21.5	0.25	1.0
*r*1–*s*2.25	22.5	82.6	96.9	22.5	94.5
*r*0.5–*s*2.25	22.5	82.6	96.9	11.25	47.2
*r*0.05–*s*2.25	22.5	82.6	96.9	1.125	4.7
*r*0.5–*s*4	40	146.9	172.2	20	84.0
*r*0.05–*s*4	40	146.9	172.2	2	8.4

[a] Molecular weight of 272.3 g/mol.
[b] M_n = 232 000 g/mol.
[c] M_{NaPS} = 238.2 g/mol.

2.3.1. Rheology

The viscosity of the HEC solutions was measured by a Bohlin CVO rheometer using a cone and plate, 1° and D40 mm, with a 30 μm gap. The measurements were performed using a programmed step-routine at isothermal conditions at 23 °C where the shear rate was gradually increased every 5 s (25 steps) from 1 to 1000 s^{-1}. The viscosity values reported here were recorded at a shear rate of 100 s^{-1}.

2.3.2. Molecular weight

The molecular weight of the samples withdrawn from the reactor was analyzed mainly using size exclusion chromatography (SEC) but complimentary studies were also performed using an Ubbelohde capillary viscometer.

2.3.2.1. Size exclusion chromatography. SEC equipped with a dual refractometer/viscometer detector (Viscotek Model 250) and a polymer packed column (Tosoh Biosep TSK gel $GMPW_{XL}$) at ambient temperature was used for the analysis. The mobile phase was an aqueous solution of 10 mM $NaNO_3$ (Millipore water) with a flow rate of 0.3 mL per min. The injection volume was 200 μL and the HEC concentration was 0.2 wt.%. The system was calibrated with Pullulan polysaccharide standards having a molecular weight ranging between 180 (glucose) and 1,600,000 g/mol. The response from the refractive index (RI) detector, using the Pullulan standards, was plotted as a function of the retention volume, which gave a linear calibration curve.

2.3.2.2. Ubbelohde capillary viscometer. The samples were diluted with deionized water and the specific viscosity (η_{sp}) at different concentrations (C) was then measured at 23 °C. The intrinsic viscosity ($[\eta]$) was obtained by extrapolating the linear plot of $(\eta_{sp})/C$ vs. C to zero concentration. The viscosity average molecular weight ($\bar{M}_v$) of HEC was calculated using the Mark–Houwink equation, $[\eta] = k\bar{M}_v^{\alpha}$. Two sets of constants were used and calculated M_v values were compared with the M_w results from the SEC analysis. One set of constants were taken from Polymer Handbook (Brandrup, Immergut, & Grulke, 1998), i.e. $k_1 = 9.53 \times 10^{-3}$ and $\alpha_1 = 0.87$, and the other set of constants, $k_2 = 3.73 \times 10^{-2}$ and $\alpha_2 = 0.76$, were derived from the experimental results, for further information see Section 3.

2.3.3. Iodometric titration of NaPS

The amount of persulfate remaining in the withdrawn samples was volumetrically determined using a standard iodometric method (Kolthoff & Carr, 1953). In addition to the HEC samples the decomposition of NaPS in deionized water was also studied in both non-buffered and buffered solutions using sodium hydrogen carbonate ($NaHCO_3$) as the buffer.

To 25 mL of a cooled sample (see Table 1) 4 g KI was added and the sample was sealed. The non-decomposed persulfate oxidized the added iodide according to reaction (1) and the samples were colored violet by the formation of I_2.

$$S_2O_8^{2-} + 2I^- \rightarrow 2SO_4^{\bullet -} + I_{2(aq)} \quad (1)$$

Ten minutes after the addition of KI the samples were acidified with 1 ml of 6 M CH_3COOH and a small amount of starch indicator was added. Thereafter, the samples were titrated with sodium thiosulfate ($Na_2S_2O_3$) to the starch indicator end-point, indicated by a color change from violet towards yellow and finally transparence when all iodide had reacted (2). The concentration of the $Na_2S_2O_3$ was adjusted so that the final titration volume was between 5 and 25 mL.

$$I_{2(aq)} + 2S_2O_3^{2-} \rightarrow 2I^- + S_4O_6^{2-} \quad (2)$$

3. Results and discussion

The degradation of HEC by free radicals generated by NaPS has been studied at three temperatures, three NaPS/HEC ratios and three HEC concentrations (see Table 1). The molecular weight evolution during the reactions was followed by means of rheology and SEC analyses of samples taken over the course of the reactions and the decomposition of persulfate was followed by iodometric titrations. The results from these experiments are presented and discussed below.

3.1. Rheology

The general behavior observed in all rheology measurements was a dramatic decrease in the viscosity of the HEC solutions immediately after the NaPS was added. Fig. 2a shows the decrease in viscosity with time for HEC samples degraded at 60 °C using different solids content and HEC/NaPS ratios. The largest differences in the viscosity observed were naturally dependent on the original HEC concentration used in the experiments. However, as can be seen in Fig. 2a, the initial decrease in viscosity was fast but leveled off after a relatively short time and the decrease in viscosity after 20 min was slow and in some samples the viscosity had almost reached a constant value at this point.

Fig. 2b shows the decrease in viscosity with time for HEC samples having 2.25 wt.% solids content at different temperatures and NaPS/HEC ratios. The viscosity decreased faster with increased NaPS concentration and/or temperature, which is expected since the instantaneous number of free radicals in the reaction mixture increases both with increased NaPS concentration and increased temperature. After just 10 min the highest sample viscosities of all the experiments were obtained for the experiments with the lowest NaPS/HEC ratio, i.e. 0.05. This indicates that at low NaPS/HEC ratio the NaPS concentration dominates the radical formation regardless of the reaction temperature.

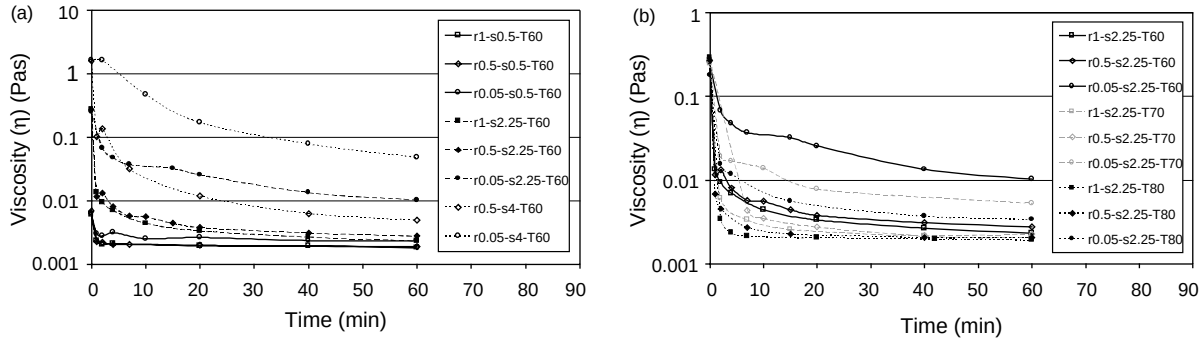

Fig. 2. (a) Viscosity of HEC samples at 60 °C using different NaPS/HEC ratios (*r*1—□, *r*0.5—◇ and r0.05—○) and solids content (*s*0.5—, *s*2.25- - - and s4…). (b) Viscosity of HEC samples having 2.25 wt.% solids content at 60, 70 and 80 °C and NaPS/HEC ratios (*r*1—□, *r*0.5—◇ and *r*0.05—○).

Apart from at the lowest NaPS/HEC ratio, the effect of reaction temperature dominated the viscosity decrease. The result was that the lowest viscosities at a given NaPS/HEC ratio were obtained in samples reacted at a temperature of 80 °C, which then increased in the order of samples reacted at 70 and 60 °C, respectively.

Kiselenko et al. (1980)showed that in the absence of atmospheric oxygen, cellulose ethers in aqueous solutions undergo no degradation for 2 h even at 70 °C. This was also the case in the present study where no degradation of HEC could be observed in either the rheology or the SEC analyses in the purged samples even after 80 °C for 2 h. The fast initial decrease in viscosity followed by a slower decrease towards an almost constant value as shown in Fig. 2a and b has also been observed in other studies where cellulose ethers have been degraded using APS or KPS (Berlin & Kislenko, 1992; Donescu et al., 1981; Kiselenko et al., 1980; Kislenko et al., 2000). The study by Kislenko et al. (2000) also showed that the initial degradation rate increased with increased initial concentration of persulfate and vice versa, with an increase in the initial concentration of the polysaccharide the degradation rate decreased. As also observed in the present study Kislenko et al. showed that the initial degradation rates were dependent on the persulfate/polysaccharide ratio. However, when experiments in the present study with NaPS/HEC ratios of 0.5 and 1, respectively, and with the same solids content were compared, there were almost no differences in the results. This can be seen in Fig. 2a for experiments *r*1–*s*0.5–T60 and *r*0.5–*s*0.5–T60 and experiments *r*1–*s*2.25–T60 and *r*0.5–*s*2.25–T60, respectively, where the viscosity as a function of the degradation time was mainly dependent on the HEC concentration in the samples and not on the NaPS/HEC ratio. This indicates that there existed a maximum value of the NaPS/HEC ratio at each temperature after which the system became saturated with persulfate radicals and any further increase of the NaPS concentration would not have increased the degradation rate of HEC. Since the average molecular weight for a glucose unit is 272 g/mol, which is similar to the molecular weight for NaPS, see Table 2, the molar concentration ratio and the weight ratio of NaPS/HEC were comparable in all experiments.

Formation of carboxylic groups (Kiselenko et al., 1980) and the incorporation of sulfate groups in the HEC molecules resulting from the degradation reaction could lead to the formation of charged polymer chains, and thereby the possibility for the HEC molecules to act as polyelectrolytes. In order to see whether the degraded HEC could be regarded as a polyelectrolyte, the ratio between the specific viscosity (η_{sp}) and the HEC concentration (C) was plotted as a function of C for degraded HEC samples as seen for *r*0.05–*s*2.25–T60–*t*7 in Fig. 3. When the η_{sp}/C is plotted as a function of C for a polyelectrolyte the curve reaches a minimum when the concentration is decreased and at even lower concentrations the values of η_{sp}/C increases (Billmeyer, 1971). This behavior was not observed for any of the investigated samples and the obtained slopes were linear as in Fig. 3 for *r*0.05–*s*2.25–T60–*t*7 and we therefore concluded that the degradation reaction of HEC most likely did not cause the formation of HEC polyelectrolytes.

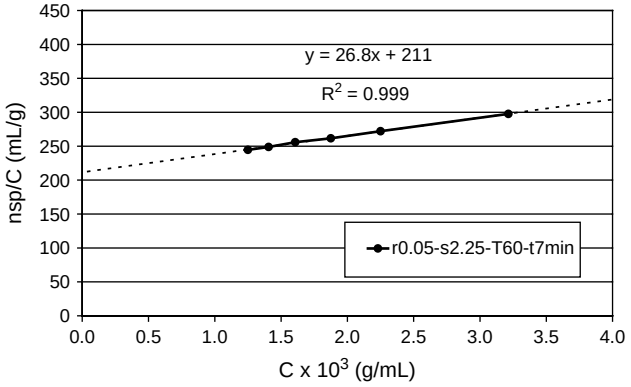

Fig. 3. The specific viscosity (η_{sp}) divided by the HEC concentration (C) as a function of C for sample *r*0.05–*s*2.25–T60–*t*7. The extrapolated η_{sp}/C intercept at zero concentration provides the intrinsic viscosity ([η]) of 212 ml/g.

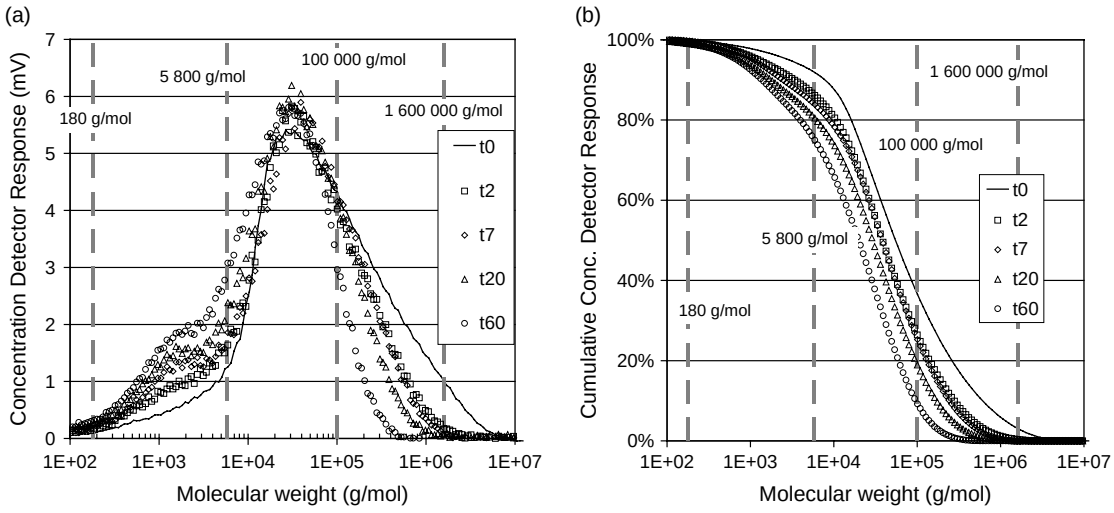

Fig. 4. (a) Molecular weight distributions at different reaction times for *r*0.05–*s*2.25–T60. (b) The CCDR as a function of the molecular weight at different reaction times for *r*0.05–*s*2.25–T60. The solid black line indicating the neat HEC. In the figures the molecular weight decreased with time when shifted towards the left.

3.2. Size exclusion chromatography

The molecular weight distributions of $r0.05-s2.25$ reacted at 60 °C, for samples taken at different reaction times, are shown in Fig. 4a and in Fig. 4b the cumulative concentration detector responses (CCDR) as a function of the molecular weight are shown. The black solid curve in both Figures represents the original HEC molecular weight distribution before the initiator was added at time 0 (t_0). The neat HEC polymer had a broad distribution with a fraction of high molecular weight material above 10^6 g/mol, see Fig. 4a. However, after the initiator was added the molecular weight started to decrease and already after 2 min the ultra-high molecular weight fraction had almost disappeared, which corresponds to the sharp initial viscosity drop in Fig. 2a for this sample. On the other hand, there was a low molecular weight fraction formed, which increased in concentration throughout the reaction. In Fig. 4b it can be seen that the reaction was rather slow and that the reaction rate was relatively constant throughout the reaction. A much higher degradation rate as compared to *r*0.05–s2.25–T60 can be observed for experiment *r*1–*s*2.25–T60 in Fig. 5a, which shows the evolution of the molecular weight distribution during reaction. Fig. 5b shows the CCDR as a function of the molecular weight at different times for $r1-s2.25$ at 60 °C.

The difference between the samples in Figs. 4 and 5 were the NaPS/HEC ratios, i.e. the relative amount of initiator present. In the experiments with a high NaPS/HEC ratio, i.e. $r=1$, the degradation reaction was fast and the molecular weight distribution developed differently as compared with the experiments in which the ratio was low, i.e. $r=0.05$, where the degradation rate was slow and the molecular weight decrease from (M_{w0}) 230,000 g/mol to (M_{w60})

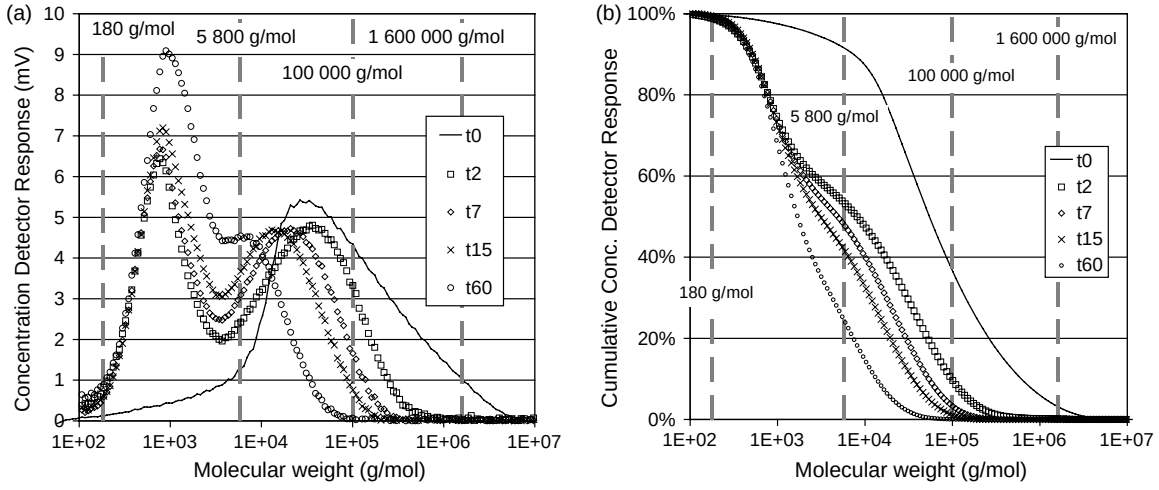

Fig. 5. (a) Molecular weight distribution at different reaction times for *r*1–*s*2.25–T60. (b) The CCDR as a function of the molecular weight at different reaction times for *r*1–*s*2.25–T60. The solid black line indicating the neat HEC. In the figures the molecular weight decreased with time when shifted towards the left.

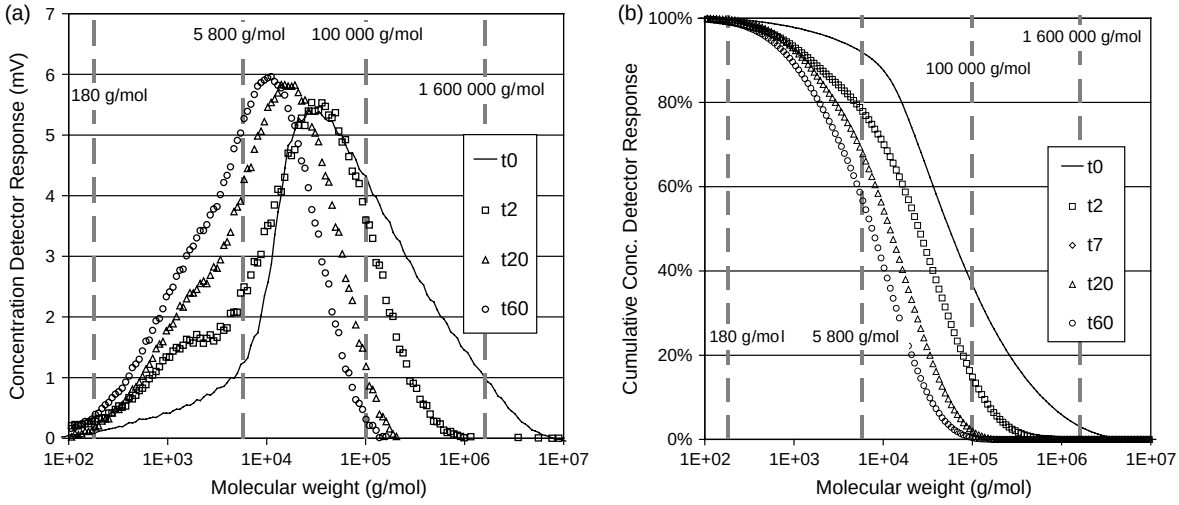

Fig. 6. (a) Molecular weight distributions at different reaction times for *r*0.05–*s*2.25–T80. (b) The CCDR as a function of the molecular weight at different reaction times for *r*0.05–s2.25–T80. The solid black line indicating the neat HEC. In the figures the molecular weight decreased with time when shifted towards the left.

40,000 g/mol occurred at a rate low enough to be controlled. In experiment *r*1–*s*2.25–T60 a large quantity of low molecular weight polymer was formed instantly when the degradation reaction started and after 2 min there was a considerable amount of material generated with molecular weight below 1500 g/mol, as can be seen in Fig. 5a. However, there was simultaneously also present in the reaction mixture a high concentration of larger molecules with molecular weights well above 20,000 g/mol and the sample molecular weight distribution changed from being broad monomodal towards having two narrow peaks, i.e. a bimodal distribution developed over the course of the reaction.

Fig. 6a and b show the molecular weight distributions and CCDR, respectively, at different reaction times for *r*0.05–*s*2.25–T80. The difference between the experiments reported in Figs. 4 and 6 was that the temperature was increased from 60 to 80 °C. The degradation for the samples with the higher temperature 80 °C (Fig. 6) was faster compared to the 60 °C samples (Fig. 4). However, even if the degradation reaction was faster at 80 °C the molecular weight distribution developed similarly as compared with the experiments in which the temperature was 60 °C, i.e. no bimodal M_w distribution was observed.

The CCDR as a function of the molecular weight at different ratios, solids content and temperature at the reaction

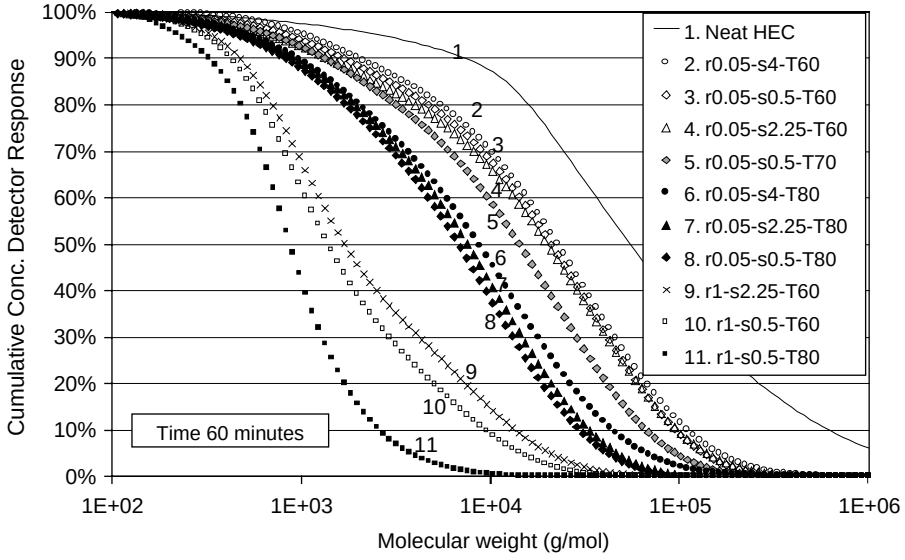

Fig. 7. The CCDR as a function of the molecular weight at different ratios, solids content and temperature at the reaction time 60 min. The neat HEC is included as a reference as curve no 1. The figure legends are listed in descending order depending on the degree of degradation. Symbols indicating NaPS/HEC ratio (*r*) and solids content (*s*) as follow: *r*0.05 − *s*4 (○), *r*0.05 − *s*2.25 (△), *r*0.05 − *s*0.5 (◇), *r*1 − *s*2.25 (×) and *r*1 − *s*0.5 (□). In the case of where applicable the symbols represent temperature: Open—60 °C, filled grey—70 °C and filled black—80 °C.

time 60 min are shown in Fig. 7, the neat HEC is given as a reference. The results show that the degradation of HEC proceeded faster when the NaPS concentration was increased, i.e. increasing NaPS/HEC ratio from *r*0.05 to *r*1. This was clear from comparing the molecular weight at 50% CCDR for *r*0.05–*s*0.5–T60–*t*60 (curve 3), value 20,900 g/mol, with *r*1–*s*0.5–T60–*t*60 (curve 10), value 1400 g/mol, indicating a molecular weight almost 15 times higher with the lower NaPS/HEC ratio. Sample *r*0.05–*s*2.25–T60 (curve 4) had a 12 times higher M_w compared with *r*1–s2.25–T60 (curve 9) and *r*0.05–*s*0.5–T80 (curve 8) had an 8 times higher M_w compared with *r*1–*s*0.5–T80 (curve 11) at 50% CCDR.

The results in Fig. 7 indicate that the solids content could have a small effect on the degradation reaction where the HEC will become less degraded when the solids content is increased. However, solids content at a low level (up to 2.25%) seems not to have a significant influence on the degradation rate in the parameter ranges that have been used. No clear difference between solids content 0.5 and 2.25 was observed, except at the highest ratio of 1, while the samples with the highest solids content, i.e. 4 wt. %, seem to have a slightly higher molecular weight after 60 min.

The mono- and bimodal distribution that was obtained in the SEC analyses when the NaPS/HEC ratio was changed from 0.05 to 1 could be due to mechanistic effects, a statistical effect or a combination thereof. What was evident from the SEC results was that the degradation of the HEC with low ratio seemed to occur randomly since the shape of the curves was similar to that for the neat HEC, i.e. the curves for the degraded HEC with NaPS/HEC ratio 0.05 have simply been shifted to the left in Fig. 7. The HEC molecules have been degraded without a large increase in the number of low molecular weight molecules. However, in the case of higher NaPS/HEC ratio the shape of the curves differed compared to the neat HEC, as large amounts of small molecules were formed much faster than with the lower NaPS/HEC ratio. This indicated that the reaction mechanism was not random in the case of higher NaPS/HEC ratio; instead some of the probable reaction sites tend to react more easily than others.

Most likely there exist at least two type of reactions involving the radicals and HEC where, depending on the circumstances, one or other of the reactions dominates depending on the NaPS/HEC ratio, e.g. in the case of a high concentration of NaPS the reaction causing a bimodal distribution is favored. Several reaction mechanisms are possible and in the next paper we will discuss this in detail.

The results in Fig. 7 also show that the degradation increased with temperature by comparing the samples *r*0.05–*s*0.5–T60 with *r*0.05–*s*0.5–T70 and *r*0.05–*s*0.5–T80 having a 1.5 and 3 times higher M_w, respectively. However, there was no indication that the mechanism was changed when the temperature was increased from 60 to 80 °C, except that the rate of degradation was greater.

3.3. Relationship between M_w and viscosity

The results from the previous paragraphs show that it is possible to study the degradation of HEC using rheology measurements and SEC. The advantage of rheology methods over SEC is that they are often more convenient and faster to use. However, the SEC gives important information i.e. correct molecular weight and molecular weight distribution. Phenomena such as bimodal systems, as were observed for samples with a high NaPS/HEC ratio, cannot be observed using only rheology measurements. The SEC results showed that it was not simple to convert the viscosity data to molecular weights since the molecular weight distributions for the different samples often differ largely. For example, the molecular weights for *r*0.05–*s*2.25–T60–*t*60 and *r*1–*s*2.25–T60–*t*2 had almost the same M_w (36,000 g/mol) and normalized viscosity 0.04, however, the molecular weight distributions showed a very different appearance, see Figs. 4a and 5a.

When the degradation reactions for the experiments having different NaPS/HEC ratios were compared there were indications that the degradation differed depending on the initiator concentration at a given HEC concentration. In the cases where the initiator concentration was high the fraction of low molecular weight material at a given reaction time increased non-linearly, in addition the degradation products were also smaller than in the corresponding experiments having lower initiator concentrations. As can be seen in Fig. 5b, after only 2 min of reaction almost 40% of the molecules have a molecular weight on the order of 1000 g/mol, which corresponds to about four substituted glucose units.

Nevertheless, in spite of these differences, it would be desirable if the rheology results could be transformed to

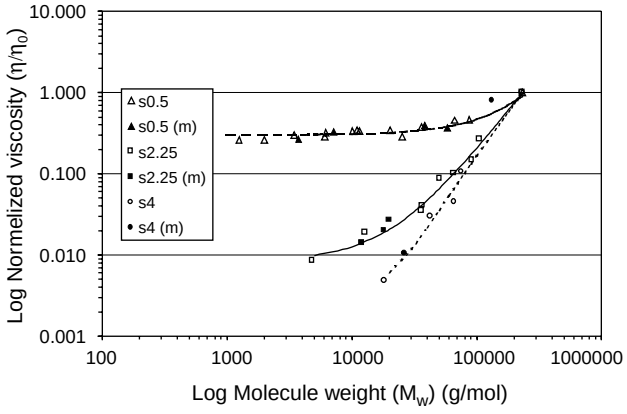

Fig. 8. Normalized viscosity as a function of the average molecular weight (M_w) for solids content 0.5, 2.25 and 4. Open symbols indicate experimental values for both the normalized viscosity and the M_w. Filled symbols indicate experimental values regarding only the M_w where the viscosity values were extrapolated from Fig. 2 and similar curves. The curves can be used to determine the molecular weight for other samples using only normalized viscosity from rheometer experiment under these conditions specified in Section 2 used in this study.

Table 3
Obtained constants from curve fitting regression, for modeling normalized viscosity as a function of the average molecular weight (M_w SEC) at different solids content

Solids content	Constants[a]			R^2
	A	B	C	
0.5	0.298	1.00×10^{-6}	7.00×10^{-12}	0.86
2.25	0.008	2.90×10^{-7}	1.72×10^{-11}	1.00
4[b]	0.007	-4.34×10^{-7}	2.03×10^{-11}	1.00

[a] Equation $y = A + B * x + C * x^2$.
[b] Sample r0.05–s2.25–T60–t4 deviated too much and was excluded in the curve fitting regression.

molecular weight and vice versa and an empirical model for doing this is presented below.

In Fig. 8 the normalized viscosity is plotted as a function of the average molecular weight (M_w SEC results) for solids content 0.5, 2.25 and 4 wt%. The viscosity was normalized by taking the viscosity of the neat HEC at t_0 to be 1. The results in Fig. 8 show that the solids content dominates and it was not possible to compare the results in respect to normalized viscosity when using different solids contents. However, the samples with the same solids content correlate with each other independently of temperature and NaPS/HEC ratio, and the plots can be used to determine the average molecular weight for other samples having these solids contents, using only the normalized viscosity from rheometer experiments. The equation obtained has the following form, $y = A + B^*x + C^*x^2$, and the constants for each solids content are presented in Table 3.

In Table 4 the intrinsic viscosity ([η]) for some of the samples calculated from the specific viscosity (η_{sp}) using an Ubbelohde capillary viscometer are presented. As a comparison the M_w from the SEC analyses were also included in Table 4. By using the Mark–Houwink equation it was possible to calculate the viscosity average molecular

Table 4
Intrinsic viscosity ([η]), viscosity average molecular weight ($\bar{M}_v$), M_n, M_w and the polydispersity index (M_w/M_n) from the SEC analyses

Time (min)	Sample	[η] (ml/g)	M_{v1} (g/mol)	M_{v2} (g/mol)	M_n (g/mol)	M_w (g/mol)	M_w/M_n
0	Neat HEC	424	219 974	230 679	7 771	232 269	29.9
2	r1–s0.5–T60	–	–	–	1 111	10 144	9.1
4	r1–s0.5–T60	13	4 011	2 302	1 078	11 017	10.2
10	r1–s0.5–T60	–	–	–	1 025	7 161	7.0
20	r1–s0.5–T60	–	–	–	1 069	6 217	5.8
60	r1–s0.5–T60	–	–	–	915	3 435	3.8
2	r1–s0.5–T80	–	–	–	990	6 071	6.1
7	r1–s0.5–T80	–	–	–	932	3 750	4.0
20	r1–s0.5–T80	–	–	–	777	1 983	2.6
60	r1–s0.5–T80	–	–	–	635	1 250	2.0
7	r0.05–s0.5–T60	167	75 462	67 358	–	–	–
60	r0.05–s0.5–T60	87	35 663	28 435	3 518	36 266	10.3
2	r0.05–s0.5–T70	–	–	–	4 729	87 464	18.5
10	r0.05–s0.5–T70	–	–	–	4 341	57 987	13.4
60	r0.05–s0.5–T70	79	31 734	24 862	2 950	25 271	8.6
2	r0.05–s0.5–T80	–	–	–	6 754	66 121	9.8
7	r0.05–s0.5–T80	117	50 131	42 075	2 743	38 335	14.0
20	r0.05–s0.5–T80	64	25 238	19 102	2 336	20 332	8.7
60	r0.05–s0.5–T80	60	23 445	17 549	1 877	11 530	6.1
2	r1–s2.25–T60	19	6 317	3 881	1 343	36 228	27.0
7	r1–s2.25–T60	–	–	–	1 370	18 107	13.2
15	r1–s2.25–T60	20	6 430	3 961	1 300	11 994	9.2
60	r1–s2.25–T60	–	–	–	1 042	4 825	4.6
2	r0.05–s2.25–T60	–	–	–	5 240	105 515	20.1
4	r0.05–s2.25–T60	206	96 050	88 908	–	–	–
7	r0.05–s2.25–T60	212	99 273	92 349	5 193	91 456	17.6
20	r0.05–s2.25–T60	176	80 155	72 200	3 370	65 271	19.4
60	r0.05–s2.25–T60	119	51 117	43 028	3 046	36 810	12.1
2	r0.05–s2.25–T80	–	–	–	3 283	50 612	15.4
20	r0.05–s2.25–T80	–	–	–	3 208	20 070	6.3
60	r0.05–s2.25–T80	–	–	–	2 176	12 818	5.9
4	r0.05–s4–T60	–	–	–	7 565	132 835	17.6
20	r0.05–s4–T60	–	–	–	5 768	75 289	13.1
60	r0.05–s4–T60	125	54 091	45 921	4 864	42 557	8.8
60	r0.05–s4–T70	68	26 867	20 527	–	–	–
4	r0.05–s4–T80	–	–	–	3 883	66 192	17.0
15	r0.05–s4–T80	–	–	–	3 356	26 462	7.9
60	r0.05–s4–T80	–	–	–	2 298	18 212	7.9

$k_1 = 9.53\times10^{-3}$ and $\alpha_1 = 0.87$ (Brandrup et al., 1998). $k_2 = 3.73\times10^{-2}$ and $\alpha_2 = 0.76$ (experimentally derived).

Table 5
Constants, i.e. k_2 and α_2, used in the Mark–Houwink equation to determine $\bar{M}_v$, were experimentally derived from six different set of data where number 5 (bold) gave the best curve fitting regression

Set of data	K	α	R^2	Excluded points
1	1.71×10^{-2}	0.82	0.9394	
2	3.00×10^{-2}	0.77	0.9802	*r*1–s2.25–*t*60 − *t*2
3	3.46×10^{-2}	0.76	0.9831	*r*1 − s2.25 − *t*60 − *t*2, − *t*15
4	4.15×10^{-2}	0.75	0.9888	*r*1–s2.25–*t*60–*t*2, –*t*15, *r*1–s0.5–*t*60–*t*4
5	$\mathbf{3.73\times10^{-2}}$	**0.76**	**0.9905**	*r*1–s2.25–*t*60–*t*2, –*t*15, *r*1–s0.5–*t*60–*t*4, *r*0.05–s0.5–*t*80–*t*60
6	2.69×10^{-2}	0.78	0.9823	*r*1–s2.25–*t*60–*t*2, *r*0.05–s0.5–*t*80–*t*60

weight ($\bar{M}_v$) (Brandrup et al., 1998), M_{v1} using the constants $k_1 = 9.53\times10^{-3}$ and $\alpha_1 = 0.87$. The samples for which both intrinsic viscosity and molecular weight (SEC) values existed were used in the curve-fitting regression to obtain our own experimental constant values. The regression analyses in Table 5 show how different data points affected the constant values as they were excluded. The second average M_{v2} was then calculated from our own experimental data where the constants $k_2 = 3.73\times10^{-2}$ and $\alpha_2 = 0.76$ were obtained from the set of data number 5 in Table 5, which gave the best curve fitting regression.

In Fig. 9 the intrinsic viscosity has been plotted against M_w (SEC results) for the experiments where both experiments have been performed. The M_{v2} curve, based on our own calculated constants, corresponded well with the results with the exception of sample *r*1–*s*2.25–T60–*t*2. However, the fit was not as accurate for the M_{v1} curve. The differences for the M_{v1} and M_{v2} curves emphasize that in order to establish correct high precision values the constants should be based on the actual polymer that is used.

For many polymers, M_v is 10–20% below M_w, and the Mark–Houwink equation is known to become inaccurate both for molecular weights below about 50,000 (because deviations from the straight-line relationship set in) (Billmeyer, 1971) and for samples where the molecular weight distribution is too broad (Brandrup et al., 1998). The M_v result for Sample *r*1–*s*2.25–T60–*t*2 of 5000–6000 was much too low compared to the SEC results of 36,000 to be reliable. This could be due to the relatively low molecular weight (<50,000). However, since many of the other samples in Table 4 that were in the same region with a M_w 20,000–50,000 had an acceptable correlation, it is more likely that the largest cause of the deviation for *r*1–*s*2.25–T60–*t*2 was because of the bimodal M_w distribution as shown in Fig. 5.

In summary the results in Table 4 and Fig. 9 show that it is possible to use normalized viscosity to determine molecular weights for degraded samples, e.g. as a production control, where NaPS/HEC ratios are not too high. However, to ensure that no bimodal system exists an analysis like SEC is recommended if the NaPS/HEC ratio is changed.

3.4. Titration of sodium persulfate

The thermal decomposition of persulfate in water has been investigated in several studies and most of them agree that the reaction is initiated by reaction (3) (Bartlett & Cotman, 1949; Beylerian, Vardanyan, Harutyunyan, & Vardanyan, 2002; Evans & Baxendale, 1946; Henton, Powell, & Reim, 1997; House, 1962; Kolthoff & Miller, 1951; Pryor, 1966).

$$S_2O_8^{2-} \xrightarrow{k_d} 2SO_4^{\bullet -} \quad (3)$$

However, since other studies (Adhikari, Sarkar, Banerjee & Konar, 1987; Bartlett & Nozaki, 1948; Bartlett & Cotman, 1949; Henton et al., 1997; Morris & Parts, 1968; Sarkar, Adhikari, Banerjee, & Konar, 1988; Sarkar et al., 1988) have shown that additional organic substances, like solvents, monomers, latex particles, detergents, polymers, etc. increase the rate of decomposition (R_d) for persulfate in water, the present study focused on by what magnitude HEC affected the decomposition of NaPS.

In Fig. 10a the normalized concentration of NaPS as a function of time is plotted using no HEC at 60 °C in a pH buffered system ($NaHCO_3$) and in non-pH buffered systems.

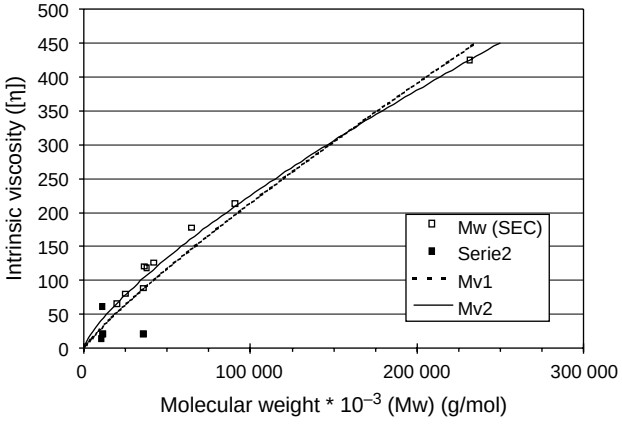

Fig. 9. Intrinsic viscosity [η] as function of the average molecular weight (M_w) and two different viscosity average molecular weight ($\bar{M}_v$) using two sets of constants, i.e. $k_1 = 9.53\times10^{-3}$ and $\alpha_1 = 0.87$; and $k_2 = 3.73\times10^{-2}$ and $\alpha_2 = 0.76$, respectively. The symbols indicate experimental data where the filled symbol show samples that have not been included in the curve fitting regression of M_{v2}.

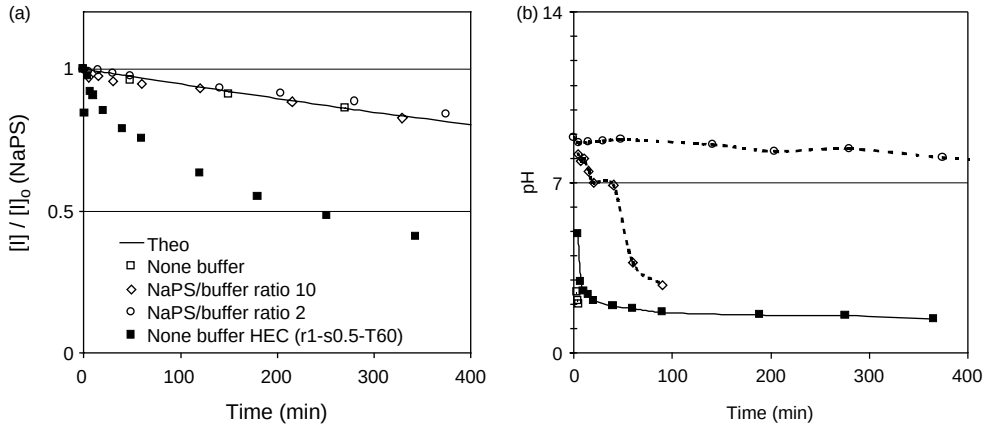

Fig. 10. (a) Normalized NaPS as a function of time for non buffered (□), NaPS/buffer ratio of 10 (◇) and 2 (○) and $r1-s0.5$-T60 (■) at 60 °C. The initial NaPS concentration of 0.021 mol/l was the same in all experiments in the figure. The solid line corresponds to the theoretical decomposition of NaPS. (b) PH as a function of time for non-buffered (□), NaPS/buffer ratio of 10 (◇) and 2 (○) and $r1-s0.5$-T60 (■) at 60 °C.

The decomposition rate coefficients have been denoted k_{dtheo} and k_{dexp}, which refers to the theoretical value for NaPS thermal decomposition in pure water found in the literature and the experimental values determined in this study. The solid line in the Fig. 10a corresponds to k_{dtheo} in pure water at 60 °C using the rate coefficient for thermal decomposition, $9.2\times10^{-6}\ \mathrm{s}^{-1}$ (Henton et al., 1997). Most probably there exist several different reactions which influence the decomposition of the persulfate, thus all have different rate coefficients. However, the presented rates of decomposition have been simplified into one single value since the purpose in the present study was only to show the overall trends and differences and not the exact decomposition mechanism. The results in Fig. 10 show that k_{dexp} of sodium persulfate in pure water at 60 °C was in accordance with the theoretical value in non-pH buffered as well in pH buffered systems. However, in the presence of HEC the decomposition rate was much higher as can be seen for experiment $r1$–s0.5–T60 in Fig. 10a. The initial rate coefficient for thermal decomposition was $2.0\times10^{-4}\ \mathrm{s}^{-1}$ (0–7 min), which was an increase of more than 20 times the theoretical value. The half-life time at 60 °C was reduced by a factor of more than five from 21 h down to 4 h in the presence of HEC.

In Fig. 10b the pH as a function of time is shown for the samples presented in Fig. 10a. In the absence of buffer or when a NaPS/buffer ratio of 10 was used, the pH decreased rapidly from 7 down to 2. The system was buffered over the time period of 400 min. when a NaPS/buffer ratio of 2 was used, i.e. a molar ratio of at least 5 was needed to buffer the system. The effect of pH in aqueous solutions on the decomposition rate of persulfate has been debated (Adhikari et al., 1987; Bartlett & Cotman, 1949; Fronaeus & Ostman, 1955; Fronaeus &

Table 6
Theoretical (k_{dtheo}) and experimentally (k_{dexp}) decomposition rates coefficients for NaPS

Theory (°C)	$k_{\mathbf{d}_{\mathrm{theo}}}(\mathrm{s}^{-1})$		$t^{1/2}_{\mathrm{theo}}$ (h)			
60	9.17×10^{-6}		21.00			
70	2.92×10^{-5}		6.59			
80	9.17×10^{-5}		2.10			
Experimental	$k_{\mathbf{d}_{\mathrm{exp}}}$ (s^{-1})		$(\mathbf{k}_{\mathbf{d}_{\mathrm{exp}}}/\mathbf{k}_{\mathbf{d}_{\mathrm{theo}}})$		$t^{1/2}_{\mathrm{exp}}$ (h)	Factor
	Initial[a]	End[b]	Initial	End		$t^{1/2}_{\mathrm{theo}}/t^{1/2}_{\mathrm{exp}}$
$r1-s0.5-t60$	1.97×10^{-4}	4.37×10^{-5}	21.5	4.8	3.9	5.4
$r0.5-s0.5-t60$	2.36×10^{-4}	4.95×10^{-5}	25.7	5.4	2.9	7.2
$r0.25-s0.5-t60$	2.05×10^{-4}	5.58×10^{-5}	22.4	6.1	2.8	7.5
$r0.05-s0.5-t60$	1.74×10^{-4}	6.07×10^{-5}	19.0	6.6	2.5	8.5
$r0.05-s2.25-t60$	1.58×10^{-4}	7.84×10^{-4}	17.2	8.6	1.8	11.8
$r0.05-s0.5-t70$	4.90×10^{-4}	1.32×10^{-4}	16.8	4.5	0.8	8.5
$r0.25-s0.5-t80$	9.12×10^{-4}	2.73×10^{-4}	10.00	3.0	0.3	7.0
$r0.05-s0.5-t80$	8.35×10^{-4}	3.38×10^{-4}	9.1	3.7	0.3	6.8

[a] The initial values are calculated based on linear regression for the time between 0 and 420 s.
[b] The end values are calculated based on linear regression for the time between 2 400 and 7 200 s.

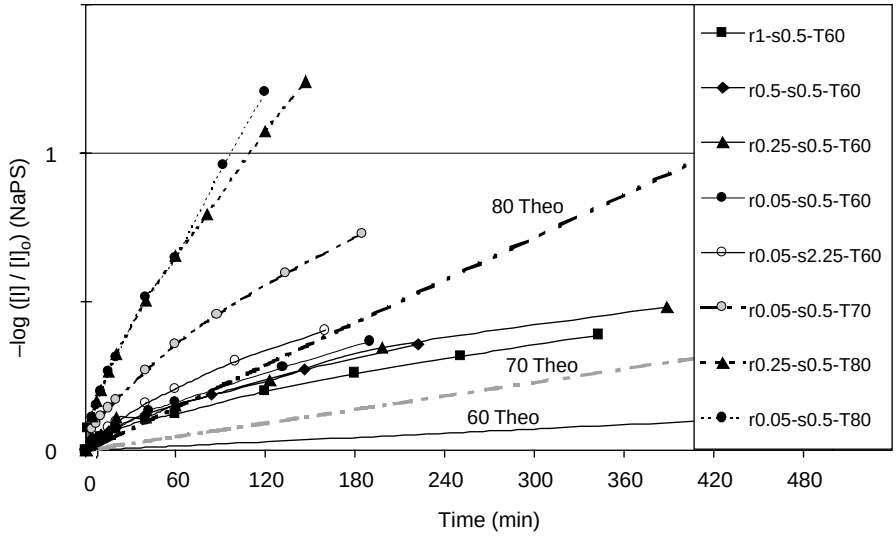

Fig. 11. Normalized rate of decomposition of NaPS as a function of time for different experiments. Dotted lines show the theoretical decomposition rates for NaPS in pure water at 60, 70 and 80 °C.

Ostman, 1968; Fronaeus, 1986; Kislenko & Berlin, 1980; Sarkar et al., 1990). It was shown that the rate of decomposition increased in acidic solutions below pH 2 (Kolthoff & Miller, 1951). When Fig. 10a and b are compared it can be seen that the decomposition rate of NaPS was independent of pH in the pH range between 7 and 2.

In Table 6 the different k_{dexp} for NaPS, obtained from Fig 11, are given together with k_{dtheo} for NaPS at the different reaction temperatures used. Since the decomposition rate was initially much higher, two different experimental values of k_{dexp} were obtained, by using linear regression, at the start of the reactions (0–420 s) and at the end of the reactions (2400–7200 s).

There were large numerical differences between the theoretical and the experimental values as can be seen by the $t^{1/2}$ ratios, see Table 6. Furthermore the results showed that the induced decomposition of NaPS differed depending on the HEC/NaPS ratios and temperatures. It was also found that the decomposition rate increased with increased concentration of HEC at a specific NaPS/HEC ratio. Generally, the decomposition rate was more pronounced at an early stage and thereafter leveled off with time towards the theoretical k_d, which also have been observed by (Morris & Parts, 1968) for vinyl monomer and surfactant containing systems. Furthermore, in the present study it was found that the decomposition rate increased with the NaPS/HEC ratio. The induced decomposition was due to the presence of HEC (see Fig. 11) and similar results have been obtained for HEC using KPS by (Kiselenko et al., 1980) and (Donescu et al., 1981). The results in Table 6 also shows that the induced decomposition was more pronounced at the lowest temperature 60 °C where the k_{dexp}/k_{dtheo} ratio was approximately 20, while at 70 and 80 °C the corresponding values were 17 and 10, respectively

4. Conclusions

When the NaPS concentration was high a bimodal molecular weight distribution with a high amount of low molecular weight HEC was obtained. It was therefore important to analyze the molecular weight of the degraded HEC by using SEC and not only by rheology, since a bimodal system was not made apparent using the later method. The SEC results show that the critical parameters were the ratio between NaPS and HEC (the NaPS concentration) and the temperature. The results indicate that there were small differences in the level of degradation due to the HEC concentration used. When all the other parameters were constant there was a trend to a small increase in the resulting molecular weight with an increase in solids content, and this applies especially for the highest solids content 4 wt.%. However, when an appropriate process with suitable parameters for the degradation of HEC has been identified, viscosity measurements might still be useful, e.g. for production control, and this study has shown that it is possible to control the degradation of HEC by using a relatively low NaPS/HEC ratio.

The iodometric titration showed that the induced decomposition of NaPS differed depending on the HEC/NaPS ratio and the reaction temperature. It was also shown that in the presence of HEC the initial decomposition of potassium persulfate was accelerated by a factor of more than 25 at 60 °C as compared to decomposition of NaPS in pure water. The decomposition of persulfate was accelerated by increased concentration of HEC and was more pronounced at lower temperatures. Finally it was also observed that the decomposition rate of NaPS was independent of pH in the range between pH 2 and 7.

Acknowledgements

VINNOVA and the industry-sponsored Centre for Amphiphillic Polymers (CAP) are gratefully acknowledged for financial support.

References

Adhikari, M. S., Sarkar, S. M., Banerjee, M., & Konar, R. S. (1987). Thermal decomposition of potassium persulfate in aqueous solution at 50 °C in the presence of ethyl acrylate. *Journal of Applied Polymer Science*, *34*(1), 109–125.

Annable, T., Gray, I., Lovell, P. A., Richards, S. N., & Satgurnathan, G. (2004). Degradation and grafting of hydroxyethyl cellulose during emulsion polymerization. *Progress in Colloid and Polymer Science*, *124*, 159–163.

Bartlett, P. D., & Cotman, J. D. (1949). The kinetics of the decomposition of potassium persulfate in aqueous solutions of methanol. *Journal of the American Chemical Society*, *71*, 1419–1422.

Bartlett, P. D., & Nozaki, K. (1948). Polymerization of allyl compounds. IV. Emulsion polymerization of allyl acetate. *Journal of Polymer Science*, *3*, 216–222.

Berlin, A. A., & Kislenko, V. N. (1992). Kinetics and mechanism of radical graft-polymerization of monomers onto polysaccharides. *Progress in Polymer Science*, *17*(5), 765–825.

Beylerian, N. M., Vardanyan, L. R., Harutyunyan, R. S., & Vardanyan, R. L. (2002). Kinetics and mechanism of potassium persulfate decomposition in aqueous solutions studied by a gasometric method. *Macromolecular Chemistry and Physics*, *203*(1), 212–218.

Billmeyer, F. W. (1971). *Textbook of polymer science* (2nd ed.). New York: John Wiley & Sons, Inc.

Brandrup, J., Immergut, E. H., & Grulke, E. A. (1998). *Polymer handbook* (4th ed.). New York: Wiley.

Craig, D. H. (1985). The effect of hydroxyethyl content on grafting reactions of hydroxyethyl cellulose during emulsion polymerization of vinyl monomers. *Polymer Materials Science and Engineering*, *53*, 529–533.

Craig, D. H. (1986). Grafting reactions of (hydroxyethyl)-cellulose during emulsion polymerization of vinyl monomers. *Advances in Chemistry Series*, *213*, 351–367.

Donescu, D., Gosa, K., Diaconescu, I., Mazare, M., & Carp, N. (1981) . Particularities of emulsion polymerization of vinyl acetate in the presence of hydroxyethylcellulose. In M. S. El-Aasser, & J. W. Vanderhoff (Eds.), *Emulsion Polymerization of Vinyl Acetate (Paper Symposium)* (pp. 203–213). New Jersey: Applied Science Publishers, Inc.

Evans, M. G., & Baxendale, J. H. (1946). A general discussion on oxidation. *Transactions of the Faraday Society*, *42*(286), 195–197.

Fronaeus, S. (1986). On the mechanism of the thermal decomposition of peroxodisulfate ion in moderately acidic solutions. *Acta Chemica Scandinavica, Series A: Physical and Inorganic Chemistry*, *A40*(9), 572–578.

Fronaeus, S., & Ostman, C. O. (1955). Kinetics and mechanism of the reaction between cerium-(III) and persulfate. *Acta Chemica Scandinavica*, *9*, 902–911.

Fronaeus, S., & Ostman, C. O. (1968). Mechanism of the thermal decomposition of peroxydisulfate ion. *Acta Chemica Scandinavica (1947–1973)*, *22*(9), 2827–2834.

Hellgren, A. C., Weissenborn, P., & Holmberg, K. (1999). Surfactants in water-borne paints. *Progress in Organic Coatings*, *35*(1–4), 79–87.

Henton, D. E., Powell, C., & Reim, R. E. (1997). The decomposition of sodium persulfate in the presence of acrylic acid. *Journal of Applied Polymer Science*, *64*(3), 591–600.

Hercules, I. (1997). *Controls flow properties of latex paints Product information: Natrosol hydroxyethylcellulose*.

House, D. A. (1962). Kinetics and mechanism of oxidations by peroxydisulfate. *Chemical Reviews*, *62*, 185–203.

Hsu, S.-C., Don, T.-M., & Chiu, W.-Y. (2001). Free radical degradation of chitosan with potassium persulfate. *Polymer Degradation and Stability*, *75*(1), 73–83.

Irwin, V. L., & Williams, M. M. (1980). Viscosity loss in hydroxyethyl cellulose thickened latex paints caused by chemical oxidants: Methods of detection. *Journal of Coatings Technology*, *52*(660), 71–74.

Janssen, B. J. W., Kroon, G., Kruythoff, D., & Salomons, W. G. (1996). *PCT: International patent Application*. California: Hercules Inc.. 47 p.

Kiselenko, V. N., Berlin, A. A., & Chernyak, B. I. (1980). Investigation of graft-copolymerization of methyl acrylate with methyl cellulose. *Journal of Applied Chemistry of the USSR*, *53*(3), 499–502.

Kislenko, V. N., & Berlin, A. A. (1980). Study of the interaction of persulfate with hydroxyethyl cellulose. *Journal of Applied Chemistry of the USSR*, *53*(9), 1530–1533.

Kislenko, V. N., Berlin, A. A., & Litovchenko, N. I. (1998). Kinetics of graft polymerization of methyl acrylate onto hydroxyethyl- and carboxymethyl cellulose. *Zywnosc, Technologia, Jakosc*, *5*(Suppl. 4), 140–146.

Kislenko, V. N., & Kuryatnikov, E. I. (2000). Kinetics of degradation of water-soluble cellulose ethers under the action of persulfate. *Russian Journal of General Chemistry (Translation of Zhurnal Obshchei Khimii)*, *70*(9), 1410–1412.

Kolthoff, I. M., & Carr, E. M. (1953). Volumetric detremination of persulfate in the presence of organic substances. *Analytical Chemistry*, *25*(2), 298–301.

Kolthoff, I. M., & Miller, I. K. (1951). The chemistry of persulfate. I. The kinetics and mechanism of the decomposition of the persulfate ion in aqueous medium. *Journal of the American Chemical Society*, *73*, 3055–3059.

Morris, C. E. M., & Parts, A. G. (1968). Decomposition of potassium peroxydisulfate in polymerization systems. *Makromolekulare Chemie*, *119*, 212–218.

Pryor, W. A. (1966). *Introduction to free radical chemistry*. Englewood Cliffs, N.J.: Prentice-Hall, Inc.

Sarkar, S., Adhikari, M. S., Banerjee, M., & Konar, R. S. (1988). Thermal decomposition of potassium persulfate in aqueous solution at 50 °C in an inert atmosphere of nitrogen in the presence of acrylonitrile monomer. *Journal of Applied Polymer Science*, *35*(6), 1441–1458.

Sarkar, S, Adhikari, MS, Banerjee, M, & Konar, RS (1990). Mechanism of persulfate decomposition in aqueous solution at 50 °C in the presence of vinyl acetate and nitrogen. *Journal of Applied Polymer Science*, *39*(5), 1061–1077.

Schwartz, M., & Baumstark, R. (2001). *Waterbased acrylates for decorative coatings*. Hannover: Vincentz.

Warson, H., & Finch, C. A. (2001). *Applications of synthetic resin latices*. Chichester: Wiley.

Winters, H. (1980). Viscosity loss in cellulosic ether-thickened latex paints caused by oxidant/reductant impurities. *Journal of Coatings Technology*, *52*(664), 71–76.